Supplementary Information: Effect of Dynamic Correlation on the Ultrafast Relaxation of Uracil in the Gas Phase

Pratip Chakraborty,[a] Yusong Liu,[b] Thomas Weinacht,[b] and Spiridoula Matsika*[a]

[a] *Department of Chemistry, Temple University, Philadelphia, Pennsylvania 19122, USA*
[b] *Department of Physics and Astronomy, Stony Brook University, New York 11794, USA.*

1 Internal coordinates of CIs

Table 1: Important internal coordinates of CIs and their energies compared to FC geometry. All CIs are ethylenic except CI21* which is a ring opening CI.

Con.Int.	**Method**	**C5=C6 (Å)**	**C4-C5 (Å)**	**C4=O8 (Å)**	**N3-C4 (Å)**	**H12C5C6H11 (°)**	**N1C6H11C5 (°)**	**C6C5H12C4 (°)**	**Energy (eV)**
FC	DFT	1.35	1.46	1.22	1.41	0	-180.0	180.0	0.0
CI21	CASSCF	1.50	1.39	1.25	1.43	-62.0	-161.7	-140.1	5.49
CI21	MRCIS	1.49	1.39	1.25	1.43	-56.4	-172.5	-150.6	5.29
CI21	XMS-CASPT2	1.42	1.43	1.26	1.47	-16.8	-174.4	-175.6	4.58
CI21	TD-DFT/TDA	1.40	1.40	1.25	1.50	25.7	-176.9	176.7	4.74
CI21*	TD-DFT/TDA	1.40	1.38	1.21	1.67	-15.09	-173.3	-177.9	4.90
CI10	CASSCF	1.43	1.52	1.19	1.42	122.9	-178.7	114.4	4.50
CI10	MRCIS	1.44	1.52	1.19	1.42	124.0	-178.2	114.7	4.37
CI10	XMS-CASPT2	1.47	1.48	1.22	1.44	114.5	-179.6	122.9	3.80

2 Additional Information on Trajectory Analysis

An important issue in TSH using multi-reference methods is that sometimes (especially after hopping to the S_0 state) trajectories fail as the active space does not converge. This can ensue if the molecule distorts significantly on the hot ground state or the proper anti-bonding orbitals are not present in the active space. This can lead to a change in the orbitals in the active space forcing an energy conservation failure for a particular trajectory. In our simulations with multi-reference methods, a fraction of the trajectories failed before the end of the respective simulation windows, after internally converting to S_0. As the fraction of trajectories in each state depends sensitively on the fraction of trajectories that crash in each state, it becomes crucial to deal with this problem. By default, trajectories are excluded from the counting once they fail. Nonetheless, using the default option, the excited state decay will appear to be slower than it is, when a significant fraction of trajectories fails on S_0. Furthermore, after hopping to the S_0 state, the PESs of S_1 and S_0 typically separate in energy by a substantial amount, rendering the probability of a back-hop low. So, it is reasonable to expect that a failed trajectory will remain on S_0 and include it in the population count. This is the approach we used in all the simulations with multi-reference methods.

A few trajectories started propagating with a wrong active space and they were excluded from all the simulations. Hence, 70, 70 and 50 trajectories were considered for CASSCF, MRCIS and XMS-CASPT2 methods, even though 71, 73 and 55 initial conditions were selected using the excitation windows, respectively. At the end of their respective simulation windows, 50, 45 and 26 trajectories survived at the CASSCF, MRCIS and XMS-CASPT2 levels, respectively.

3 Kinetic Models

Two different types of kinetic models were fitted to the populations.

3.1 Consecutive Fit

The first case is the following: $S_2 \xrightarrow{k_{21}} S_1 \xrightarrow{k_{10}} S_0$. Here, k's are the rates whereas τ's are the lifetimes ($\tau = \frac{1}{k}$). The following are the integrated equations where $[S_2]_0$ is the initial S_2 population which is 1, here.

$$S_2(t) = [S_2]_0 e^{-k_{21}t} \tag{1}$$

$$S_1(t) = [S_2]_0 \frac{k_{21}}{(k_{21} - k_{10})}(e^{-k_{10}t} - e^{-k_{21}t}) \tag{2}$$

$$S_0(t) = [S_2]_0 \left(1 + \frac{k_{10}e^{-k_{21}t}}{(k_{21} - k_{10})} - \frac{k_{21}e^{-k_{10}t})}{(k_{21} - k_{10})}\right) \tag{3}$$

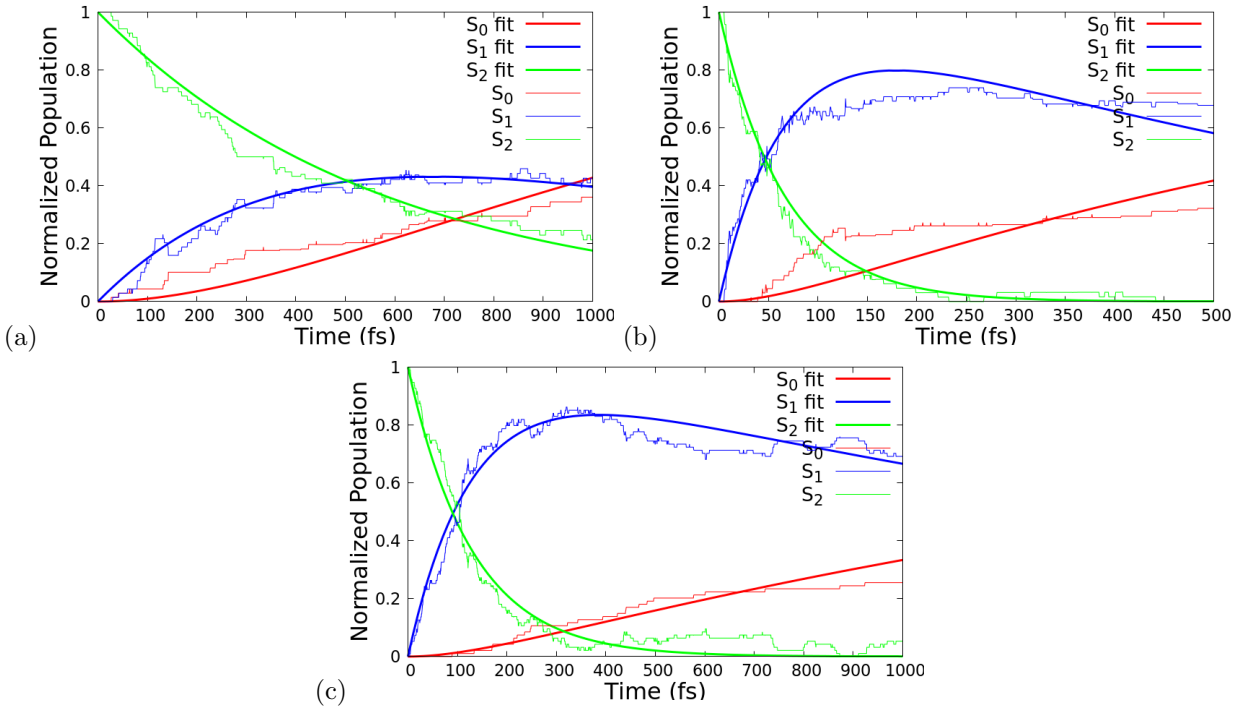

Figure 1: Consecutive fit to the S_2, S_1 and S_0 populations at the (a) CASSCF, (b) MRCIS, and (c) TD-DFT level.

Table 2: Lifetimes from the consecutive fit

Method	τ_{21}**(fs)**	τ_{10}**(fs)**
CASSCF	575.5	806.8
MRCIS	66.0	797.1
TD-DFT	129.0	2135.8

3.2 Complex fit

In this fit, another elementary rate was added to the previous fitting: $S_2 \xrightarrow{k_{20}} S_0$. The following are the integrated equations where $[S_2]_0$ is the initial S_2 population which is 1, here.

$$S_2(t) = [S_2]_0 e^{-(k_{21}+k_{20})t} \tag{4}$$

$$S_1(t) = [S_2]_0 \left(\frac{k_{21}}{k_{21}+k_{20}-k_{10}}\right)\left(e^{-k_{10}t} - e^{-(k_{21}+k_{20})t}\right) \tag{5}$$

$$S_0(t) = [S_2]_0 \left(\left(\frac{-(k_{20}-k_{10})e^{-(k_{21}+k_{20})t}}{(k_{21}+k_{20}-k_{10})}\right) - \left(\frac{k_{21}e^{-k_{10}t}}{(k_{21}+k_{20}-k_{10})}\right) + 1\right) \tag{6}$$

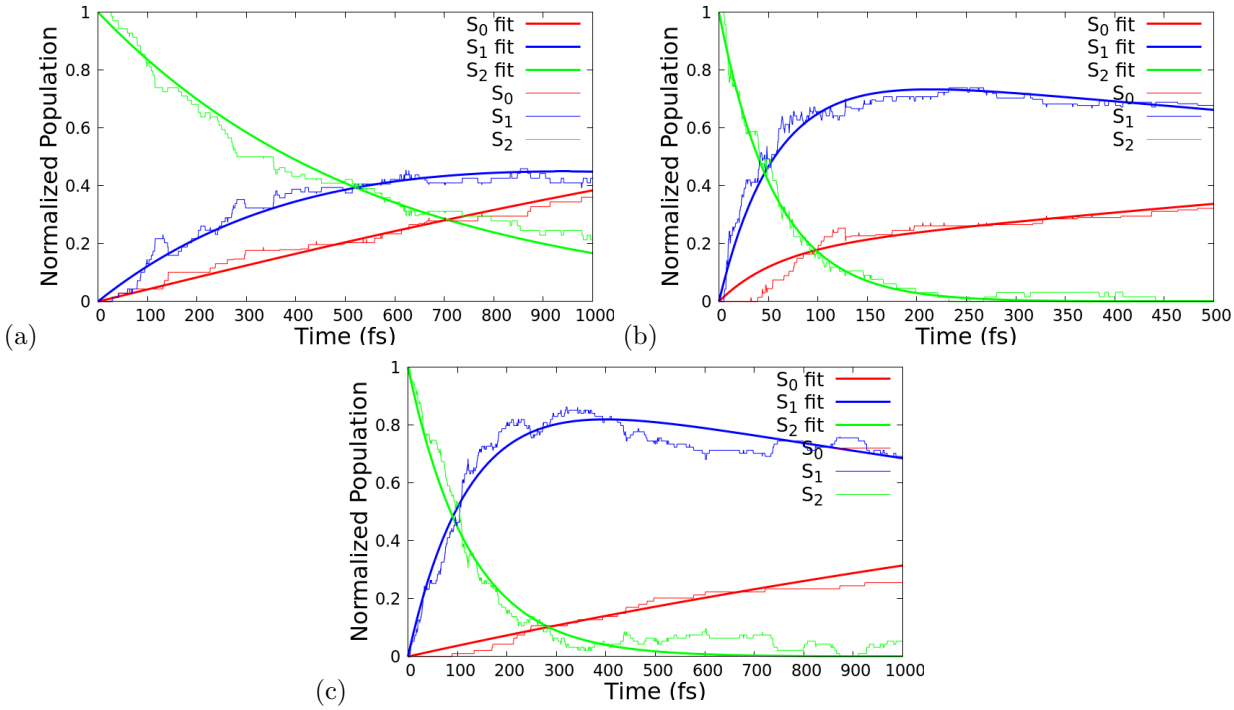

Figure 2: Complex fit to the S_2, S_1 and S_0 populations at the (a) CASSCF, (b) MRCIS, and (c) TD-DFT level.

Table 3: Lifetimes from the complex fit

Method	τ_{21}**(fs)**	τ_{20}**(fs)**	τ_{10}**(fs)**
CASSCF	728.9	2399.3	1757.4
MRCIS	70.8	292.8	2252.3
TD-DFT	130.7	2618.2	2652.0

3.3 Discussion about Kinetic Model Fits

As can be seen from Figure 1, the consecutive fit is just not good enough kinetic model for the relaxation of uracil. It fits quite well to the S_2 population, since S_2 decay is mostly exponential, and the integrated equation for S_2 is only dependent on k_{21} or τ_{21}. However, the other two states do not fit well, especially, S_0. The failure of this model means that the underlying process is more complex than two simple consecutive elementary reactions. This

is actually evident from our detailed dynamics as we have discussed in the text. In an effort to see if we can find a better fit, we added another elementary reaction from S_2 to S_0. The physical reason for this is to try to model the direct decay of $\pi\pi^*$/ground state from S_2 through S_1 without changing the state character, which occurs fast. This model, complex fit, shown in Figure 2, fits the overall populations better than the consecutive fit, but the fit is still problematic for several reasons. The fit for S_0 state is again not very good. More importantly, the τ_{20} are quite large, thus violating our assumption that this decay will be fast. The τ_{10} lifetimes also have a huge variation compared to the values of the consecutive fit, or even fitting the S_1 population independently, that we cannot trust them to be reliable. If we further consider that the dynamics were run for 300 - 1000 fs, and we are trying to extrapolate to several ps, we see that the errors can be large.

The only common thing that is clear bewteen the two fits is that the S_2 decay is exponential and the fits to S_2 are very similar with both techniques. However, since the consecutive S_2 fit is independent of any other rates except k_{21}, we will use the corresponding lifetime τ_{21} in table 2 as lifetime of S_2 at the CASSCF, MRCI and TD-DFT levels.

The populations dynamics at the XMS-CASPT2 level are far more complex because of the presence of initial population on both S_2 and S_1, and the aforementioned kinetic models fail spectacularly. Hence, we fit an exponential $0.34e^{-kt}$ to the S_2 population at the XMS-CASPT2 level to get a lifetime of 12.5 fs. The initial population on S_2 state is 0.34 at this level.

4 Bootstrapping Analysis

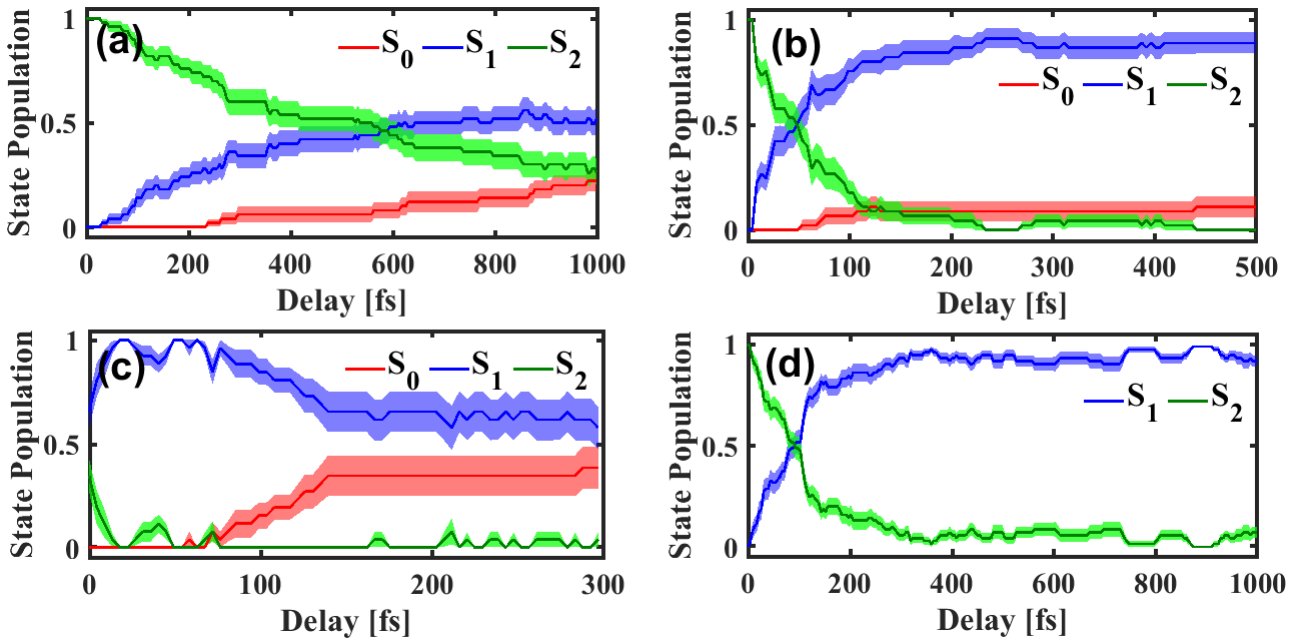

Figure 3: Bootstrapping analyses for state populations at the (a) CASSCF, (b) MRCIS, (c) XMS-CASPT2, and (d) TD-DFT level.

We have carried out a standard bootstrapping analysis on our trajectories to check if the number of trajectories is enough to provide a representative picture of what is happening at each level of theory. For this, we only used the trajectories that continued without crashing till the end of the simulation, at each level of theory. Hence, only 50, 45, 26, and 70 trajectories were used at the CASSCF, MRCIS, XMS-CASPT2, and TD-DFT level. For each level of theory, trajectories were resampled 100 times, with all the chosen trajectories randomly selected each time, generating 100 bootstrapping datasets using the standard bootstrapping method. The population of the states was estimated from each individual dataset and the standard deviation was then calculated from all datasets. We found that the standard deviation stopped increasing after using 40 bootstrapped datasets and these standard deviations are treated as the error. These errors are shown by using green, blue and red bars surrounding the S_2, S_1, and S_0 populations, respectively. One thing to note is that, we only included the raw populations here, so there is no S_0 state at the TD-DFT level. This analyses shows that even though we have a small number of trajectories, we do get a distinctive representative picture of what is happening at each level of theory very well. The small differences with the populations in the manuscript arise since we do take into account the trajectories when they fail on S_0 state in the population in the main manuscript. In general, the statistical errors from bootstrapping do not take into account how we treat failed trajectories.

5 Pyramidalization of C5 and C6

Figure 4 shows the time-evolution of C5 and C6 pyramidalization for all the multi-reference methods, along with the $S_2 \rightarrow S_1$ hops and $S_1 \rightarrow S_0$ hops, for all trajectories. According to our definition of pyramidalization angles, 180° means no pyramidalization, whereas deviations from 180° suggests pyramidalization. This shows how distinct the S_2/S_1 and S_1/S_0 seams are in case of C5 pyramidalization, and not for C6 pyramidalization. Hence, the dominant motion that brings photoexcited uracil towards the CIs, in early delays, is an ethylenic C5=C6 twist with a pyramidalization of C5.

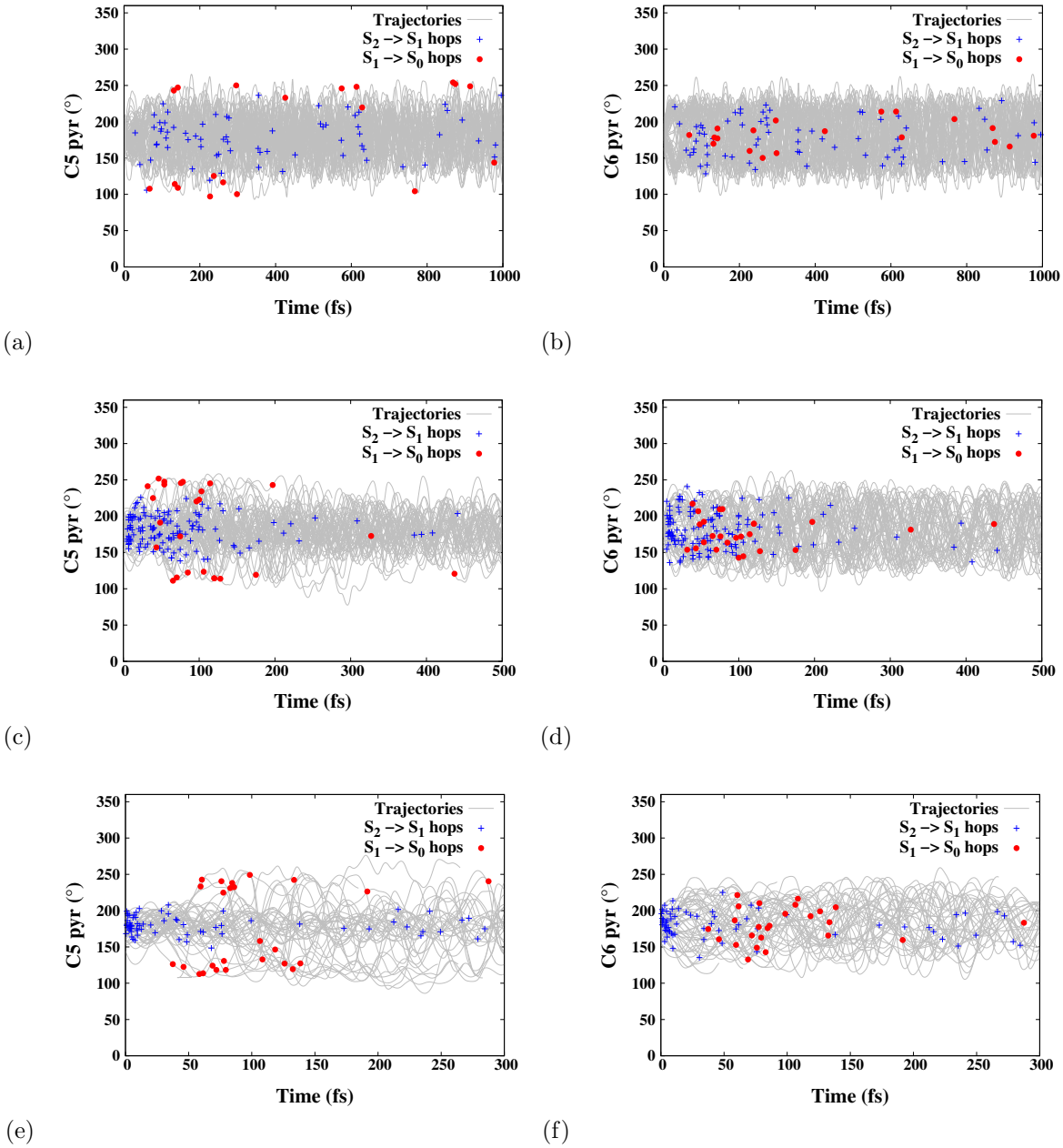

Figure 4: Time-evolution of pyramidalization at C5 (left - dihedral angle C6-C5-H12-C4) and C6 (right - dihedral angle N1-C6-H11-C5) at (a,b) CASSCF, (c,d) MRCIS, and (e,f) XMS-CASPT2 level.

6 Time-evolution of C5=C6 and C4=O8 Bonds

Figure 5 shows the time-evolution of ensemble average of the C5=C6 and C4=O8 bonds, for all the multi-reference methods. The ensemble average, in all cases, begin very close to the S_0 min value. They do not start exactly at the S_0 min, since the dynamics has been performed for a set of initial conditions and not all of them. For C5=C6 bond, it can be observed that there is rapid increase of the ensemble average towards the S_2 min value and beyond, at least for CASSCF and MRCIS methods. This sharp stretching of the bond seems very natural, since the dynamics were initiated on the S_2 surface, and the trajectories most likely traverse near the S_2 min at early times. For XMS-CASPT2 method, we have not been able to locate any S_2 min and most of the trajectories were actually initiated on the S_1 state, but the C5=C6 bond do elongate by a large amount too, demonstrating motion along this coordinate. However, this seems to change very fast for MRCIS and XMS-CASPT2 level of theory, where the ensemble average of C5=C6, contracts very quickly, within $\sim$ 150 fs, to the S_1 min value, and stays close to that value for the rest of the simulation window, which is an evidence of a population trap on the S_1 state. On the other hand, the ensemble average gradually shifts towards the S_1 min value for the CASSCF method, thereby, indicating a population trap on S_2. There is population on the S_0 state too, but a portion of those trajectories failed before the end of simulation window, owing to not satisfying the energy conservation criterion. Hence, internal coordinate information from those trajectories are not available after their failure, biasing the ensemble average towards the S_1 min value. A very similar situation can be recognized for C4=O8 bond too. In this case, the S_1 min value is larger than S_2 min, so the bond mostly stretches during the simulation window. The ensemble average of C4=O8 converges on the S_1 min value for MRCIS method, since S_1 is largely populated at 500 fs, at this level, whereas, for CASSCF, there is population on all states at the end of the 1000 fs, which is why it does not converge on the S_1 min value. For XMS-CASPT2 level, the ensemble average of C4=O8 stretches, but does not reach the S_1 min value. It, rather, averages out quickly, showing the population branching between S_1 and S_0. This is because in this case, the branching between S_1 and S_0 is almost equal, while in CASSCF and MRCIS there is smaller S_0 population at the end of the simulation, so the internal coordinates at the excited states dominate the average bond length. These observations would be important in interpreting experimental signals.

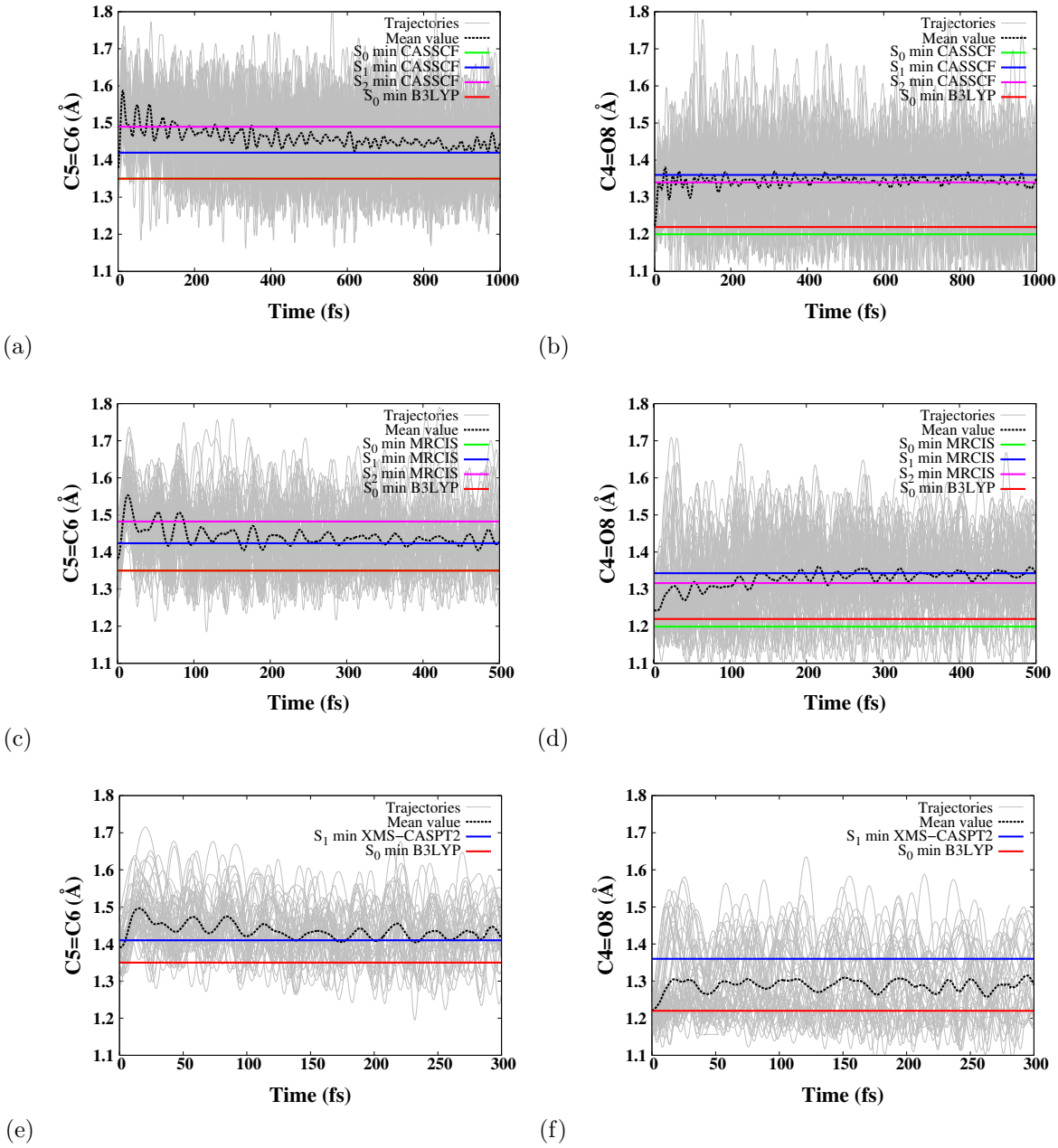

Figure 5: Time-evolution of C5=C6 and C4=O8 bonds for CASSCF(12,9)/cc-pVDZ (panel (a) and (b)), MRCIS/CAS(12,9)/cc-pVDZ (panel (c) and (d)), and XMS-CASPT2/CAS(12,9)/cc-pVDZ (panel (e) and (f)) level.

7 Cartesian Coordinates (Å) of Important Geometries

The atom numbering is different here from the conventional numbering that is provided in the manuscript.

7.1 Optimized S_0 minimum geometry of uracil at B3LYP/6-31G(d)

N -0.984401 -0.053283 0.000000
N 0.960907 1.201764 0.000000
C -0.434136 1.218141 0.000000
C 1.711123 0.048104 0.000000
C 1.138766 -1.174498 0.000000
C -0.315850 -1.298502 0.000000
O -0.950961 -2.339656 0.000000
O -1.080939 2.248655 0.000000
H -1.997745 -0.090061 0.000000
H 1.397540 2.113171 0.000000
H 2.785817 0.195528 0.000000
H 1.726741 -2.082124 0.000000

7.2 Geometries at the CASSCF(12,9)/cc-pVDZ level

S_0 minimum
N -0.983797 -0.053615 0.000000
N 0.954506 1.203664 -0.000000
C -0.421412 1.198730 -0.000000
C 1.707133 0.049966 0.000000
C 1.138302 -1.171069 -0.000000
C -0.321953 -1.284139 -0.000000
O -0.933153 -2.315485 -0.000000
O -1.067947 2.207039 -0.000000
H -1.984288 -0.078340 -0.000000
H 1.386916 2.101820 -0.000000
H 2.777017 0.192441 0.000000
H 1.723645 -2.075403 0.000000

S_1 minimum
N 0.158370 0.470453 0.092215
N 2.111540 1.729710 0.043915
C 0.745424 1.722793 -0.001746
C 2.921527 0.584275 0.145881
C 2.280803 -0.675436 0.052299
C 0.918159 -0.695604 0.005456
O 0.157368 -1.822899 0.015092
O 0.084911 2.717576 -0.104585
H -0.803176 0.447345 -0.178594
H 2.523384 2.637500 0.054370
H 3.974380 0.724345 -0.028056
H 2.848281 -1.591949 0.050021

S_2 minimum
N 0.050968 -0.131080 0.036907
N -1.255521 -2.018089 0.040436
C -1.231805 -0.657526 -0.009038
C -0.174318 -2.872791 -0.019060
C 1.160828 -2.219499 -0.086591
C 1.196131 -0.856312 0.019227

O 2.264007 -0.042116 0.073268
O -2.208923 0.040162 -0.052525
H 0.127930 0.865580 0.097873
H -2.178262 -2.401485 0.097613
H -0.322339 -3.822826 0.480930
H 2.064958 -2.798584 -0.135318

S_2 transition state
N -0.003634 0.002956 1.357411
N 1.187378 -0.516608 -0.540678
O -0.910389 0.314598 -0.717095
O 0.930120 0.405783 3.346542
C 0.004778 0.003772 -0.002502
C 1.154281 0.004555 2.146224
C 2.342785 -0.254919 1.523662
C 2.261859 -0.866873 0.166003
H -0.863943 0.249665 1.804434
H 3.284552 0.059268 1.939718
H 2.788406 -1.755954 -0.173879
H 1.087846 -0.798992 -1.500812

S_1/S_0 ethylenic CI
N -0.684383 -0.226646 -0.021570
N 0.703804 1.653582 0.137522
C -0.595403 1.108661 0.257491
C 1.748121 0.862657 -0.122770
C 1.703948 -0.506090 0.295769
C 0.397934 -1.136062 -0.144592
O 0.183088 -2.258287 -0.467117
O -1.524310 1.824104 0.482260
H -1.613600 -0.585737 -0.125773
H 0.723824 2.647792 0.000905
H 2.566915 1.326649 -0.665418
H 1.560417 -0.490467 1.390444

S_2/S_1 ethylenic CI
N -0.930569 -0.060379 0.319942
N 1.003293 1.157803 -0.112661
C -0.407735 1.137817 -0.090508
C 1.683679 0.102079 0.356314
C 1.109516 -1.216689 -0.069858
C -0.274234 -1.274036 -0.049189
O -1.031394 -2.193084 -0.431298
O -1.029806 2.129285 -0.340187
H -1.931892 -0.090500 0.296835
H 1.399142 2.077121 -0.200907
H 2.678725 0.256598 0.742735
H 1.608201 -1.712060 -0.896499

7.3 Geometries at the MRCIS/CAS(12,9)/cc-pVDZ level

S_0 minimum
N -0.980003 -0.053767 0.000000
N 0.952831 1.199884 0.000000
C -0.420114 1.201316 0.000000

C 1.704073 0.052980 0.000000
C 1.134393 -1.171138 0.000000
C -0.323403 -1.285235 0.000000
O -0.940512 -2.313198 0.000000
O -1.069372 2.211008 0.000000
H -1.981581 -0.077578 0.000000
H 1.385562 2.099239 0.000000
H 2.773772 0.198155 0.000000
H 1.721214 -2.074428 0.000000

S_1 minimum
N -0.991788 -0.065973 0.109108
N 0.943506 1.199658 0.028508
C -0.418499 1.191556 0.030168
C 1.758398 0.065140 0.154048
C 1.116256 -1.198298 0.017833
C -0.239938 -1.223216 -0.005613
O -0.999304 -2.329763 -0.055924
O -1.092382 2.185896 -0.016446
H -1.975967 -0.091092 -0.063856
H 1.349499 2.110993 0.062570
H 2.797232 0.208215 -0.097966
H 1.686565 -2.112111 -0.021030

S_2 minimum
N 0.045426 -0.126983 0.035055
N -1.244667 -2.017383 0.040748
C -1.234588 -0.654941 -0.001664
C -0.172866 -2.869129 -0.030135
C 1.157756 -2.216412 -0.063254
C 1.206645 -0.861187 0.009331
O 2.248749 -0.057230 0.016322
O -2.225839 0.028730 -0.047316
H 0.132916 0.870233 0.089689
H -2.169246 -2.402132 0.095422
H -0.336807 -3.837881 0.428471
H 2.058878 -2.797754 -0.144802

S_2 transition state
N -1.006553 -0.043453 0.050591
N 0.963284 1.165371 0.054945
C -0.437820 1.172519 0.070716
C 1.786651 0.108662 0.132304
C 1.096127 -1.207617 0.031528
C -0.295375 -1.292877 0.004773
O -1.008705 -2.295336 -0.026661
O -0.998216 2.247439 0.098218
H -2.005852 -0.089979 0.037516
H 1.341410 2.097399 0.028721
H 2.820218 0.277131 -0.136656
H 1.678160 -2.112719 0.015235

S_1/S_0 ethylenic CI
N -0.677895 -0.215513 -0.070531
N 0.709601 1.657670 0.172576
C -0.594712 1.106957 0.256208

C 1.734234 0.871834 -0.139073
C 1.719333 -0.507424 0.259270
C 0.393325 -1.153791 -0.091218
O 0.153064 -2.308673 -0.225101
O -1.521050 1.824624 0.487182
H -1.607989 -0.578503 -0.147232
H 0.721853 2.654657 0.040145
H 2.525246 1.341196 -0.718854
H 1.615069 -0.520652 1.358001

S_2/S_1 **ethylenic CI**
N -0.937764 -0.055475 0.301353
N 0.989693 1.167015 -0.098881
C -0.409367 1.148279 -0.071861
C 1.705583 0.097678 0.308949
C 1.109622 -1.211644 -0.061634
C -0.274377 -1.271470 -0.050935
O -1.028050 -2.203697 -0.408502
O -1.036954 2.149010 -0.300761
H -1.938504 -0.088886 0.255557
H 1.381691 2.091053 -0.160992
H 2.673010 0.261767 0.756823
H 1.645565 -1.865782 -0.735166

7.4 Geometries at the XMS-CASPT2/CAS(12,9)/cc-pVDZ level

S_1 **minimum**
N -0.9948359760 -0.0661707980 0.1093664956
N 0.9539975607 1.2029854628 0.0278121381
C -0.4230341162 1.2095299207 0.0020264746
C 1.7687759696 0.0569806338 0.0426623281
C 1.1364519401 -1.2067342685 0.0358303415
C -0.2395948607 -1.2440655273 0.0477172563
O -1.0212252184 -2.3510254808 0.0474235371
O -1.1056074783 2.2194185276 -0.0824366301
H -1.9990097821 -0.0969321970 -0.0435494665
H 1.3680499456 2.1272596507 -0.0381081086
H 2.8450910919 0.2132063518 0.0444223756
H 1.7139746292 -2.1306893855 0.0303571044

S_1/S_0 **ethylenic CI**
N -0.6540906176 -0.1900692443 -0.1564480221
N 0.7690495379 1.6605224436 0.2091301270
C -0.5733700653 1.1387753138 0.2145063672
C 1.7713007319 0.8381523453 -0.1650908536
C 1.6721560854 -0.5405898754 0.3346035412
C 0.3701141255 -1.1874177426 0.0469234094
O 0.0492679712 -2.3603631594 0.0919251328
O -1.5121508552 1.8840008902 0.4147167674
H -1.6080496763 -0.5520386426 -0.1829790555
H 0.7982511045 2.6785992843 0.1032723351
H 2.5654337468 1.2479142316 -0.8055197032
H 1.7761481902 -0.5350443605 1.4393577018

S_2/S_1 **ethylenic CI**

N -0.9842290917 -0.0593279921 0.3201730704
N 0.9384953155 1.2018389398 -0.0807039440
C -0.4618301690 1.1547391874 -0.0818437322
C 1.7594414328 0.1122064089 0.2336217165
C 1.1640367163 -1.1612632941 0.0616048789
C -0.2566662887 -1.2880729801 -0.0286092075
O -0.9365997088 -2.2733040675 -0.4107469780
O -1.1121187743 2.1664328198 -0.3588497527
H -1.9847125089 -0.1314835355 0.1248221349
H 1.3251693332 2.1238824698 -0.2897365200
H 2.7974346587 0.3161312287 0.4994478796
H 1.7755186669 -2.0559667469 -0.0784524683

7.5 Geometries at the TD-DFT/B3LYP/6-31G(d) level

S_2 minimum
N 0.058675 0.915342 0.304390
N -1.235730 -0.957587 0.005512
C -1.146593 0.376679 0.064068
C -0.072395 -1.790874 0.176577
C 1.180222 -1.184552 -0.001986
C 1.331207 0.209167 -0.057508
O 2.251940 0.962383 -0.408771
O -2.174338 1.130087 -0.091069
H 0.104012 1.929219 0.344037
H -2.092920 -1.326750 -0.388394
H -0.249104 -2.757352 0.631714
H 2.070157 -1.787802 -0.151609

S_2/S_1 ethylenic CI (TD-DFT/TDA/B3LYP)
N 0.0082323709 -0.8872902241 -0.4763507450
N -1.2018184249 0.9706025201 0.0939916162
C -1.1563676066 -0.3630527932 -0.0487887924
C -0.0076137116 1.7467317448 -0.1697278401
C 1.2285307575 1.1218626710 -0.0089174445
C 1.2944861963 -0.2801271211 -0.0037949643
O 2.1097634338 -1.1312434111 0.3995702125
O -2.1483950178 -1.1234513452 0.2324443526
H 0.0123819713 -1.8944935271 -0.6223905269
H -1.9361832414 1.3255518514 0.6979537249
H -0.1826667910 2.7539505182 -0.5216988121
H 2.1431550630 1.6818864314 0.1670985804

S_2/S_1 ring-opening CI (TD-DFT/TDA/B3LYP)
N -0.0507367764 -0.8404619729 0.5226765836
N -1.2051201950 1.0450833682 -0.1044184499
C -1.2211738176 -0.3122310453 0.0301525423
C 0.0331571840 1.7470839178 0.0962497339
C 1.2712335619 1.1233924989 -0.1151737911
C 1.4088982988 -0.2479971845 -0.0331065780
O 2.1061225100 -1.1902512989 -0.3462463688
O -2.2007974231 -1.0402289478 -0.2160152713
H -0.0752700473 -1.8570283778 0.6135586375
H -1.8697379002 1.3959752691 -0.7883338628
H -0.0796713384 2.7983768005 0.3082905435

H 2.1642932452 1.7033594567 -0.3145673224